Statistical study of Nanocristalline alloy cut-cores from two different manufacturers

Fabien Sixdenier, Julien Morand, Oriol Salvado, Dominique Bergogne

HAL Id: hal-01381386
https://hal.archives-ouvertes.fr/hal-01381386

Statistical study of Nanocristalline alloy cut-cores from two different manufacturers

Fabien Sixdenier[1], Julien Morand[2], Oriol Aviño Salvado[1], Dominique Bergogne[1]

[1]Université de Lyon, Université Lyon 1, CNRS UMR5005 AMPERE,
43, Bld du 11 Novembre 1918, Villeurbanne, F69622 FRANCE
[2]ADENEO, Adetelgroup, 4, chemin du ruisseau, Écully, F69130, FRANCE

The "classic" shape of a magnetic circuit made of nanocrystalline alloy is usually the toroidal one. In power electronics, this shape is not the best one in terms of size and congestion. For high power magnetic components, the UU or CC shape is preferred. Recently two manufacturers have commercialized new magnetic circuits made of nanocrystalline alloy in this last shape. But before using these new products in power electronics, we have, first to know them well and to be sure that they will respond adequately to the peculiar needs of the application. In this paper, we compare several cut cores geometric dimensions and magnetic properties from two different manufacturers. Full amplitude characterisations are performed. The dispersions of the samples and the agreement to datasheets are presented.

Index Terms—Magnetic materials, Magnetic cores, Magnetic losses, Transformers, Materials reliability...

I. INTRODUCTION

Since 1987 (year of Hitachi Metals patents), nanocrystalline alloys have become more and more popular due to their excellent magnetic properties (due to their ultrafine grain structure [1]). In [2] the authors chose to test a nanocrystalline material for a common-mode inductor used in a motor driven by an adjustable speed electrical power drive system. Due to their excellent magnetic properties (low losses, high μ_r and high B_s), the authors conclude that nanocrystalline materials are more suitable for common mode inductors than laminated or powder iron and ferrites. For the same application (common mode inductor) made with nanocrystalline alloy, authors of [3] developed a Cauer-Network model to predict the behaviour of the component (especially the losses), whereas the authors of [4] developed a model to represent the magnetic behaviour taking into account the temperature. Both models are in good agreement with measurements. An old but very robust application is presented in [5] where the authors use an inductor made of nanocrystalline material which present a high B_r/B_s ratio (square loop with $B_r/B_s \approx 0.9$). In [6], the authors showed that the use of nanocrystalline alloys (in replacement of NiFe wound cores) in the current transformer cores can contribute to the reduction of phase errors, improving thus the accuracy class. The application here would be a voltage transformer used in a Double Active Bridge Converter (DAB1). In [7], the authors verify the influence of some machining methods on the increase of core losses in nanocrystalline cut cores and show an approach to keep the effect minimized. Compared to ferrites, there is a lack of information in the datasheets of these cores. For example, we can only find the losses versus frequency for one level of flux density. If we consider the two principal manufacturers, Vacuumschmelze gives a curve for $B_{max} = 0.3$ T, and Hitachi Metals curve is for $B_{max} = 0.1$ T. It doesn't help to compare the materials. Moreover the losses are given on a uncut core and for a sinusoidal flux density which is not the waveform that will "see" the core in this kind of application (DAB1).

For these reasons, we have decided to make a statistical study on several cores from two different manufacturers : Hitachi Metals and Vacuumschmelze. In the next sections, the manufacturers will be called "Manufacturer A" and "Manufacturer B". First we measured the geometric dimensions and the weight of the cores and compared it to the datasheet. Then we made some magnetic measurements close to the operating conditions in terms of temperature, voltage waveform (square) and peak flux density. Measurements are statistically analysed and discussed like the author of [8] did it but for $Ni_{80}Fe_{20}$ wound toroidal cores. Finally after a choice and selection of a representative core from one manufacturer, we developed a new model based on improved General Steinmetz equation to compute the losses.

II. GEOMETRIC DIMENSIONS AND WEIGHT

A. Geometric dimensions

Geometric dimensions of the cores play a key role in the design steps. When engineers design a transformer, they chose a magnetic circuit that can contain the required number of turns (core window area) and that have the right iron cross section. Engineers, then need to be confident on the dimensions or weight mentioned in the datasheet, because they use these dimensions to design their transformer. The Figure 1 shows an example of the relevant outlines useful for the design of transformers. We measured our samples' dimensions and weight for both manufacturers and compared it to their respective datasheet.

Figure 2 shows the relative dimensions in (%) and the weight (last histogram) for the manufacturer "A" (20 samples) and manufacturer "B" (12 samples). The histogram value for measurements is the average relative value of the samples. The error bar on each histogram represents the maximum and minimum measured value of the complete set.
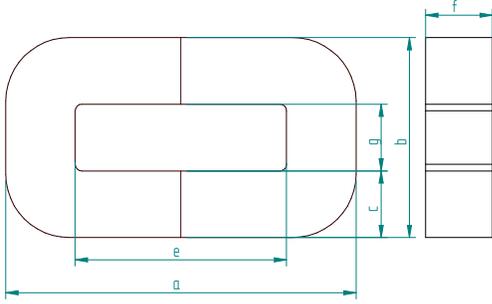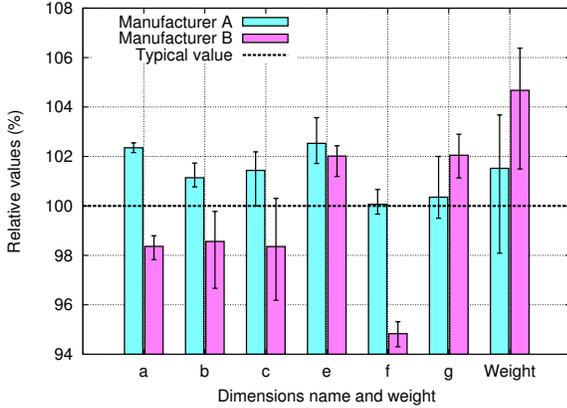
Fig. 1. Relevant outlines of the cut-cores

Fig. 2. Relative dimensions and weight for manufacturer A and B

First, all average dimensions values of the cores of manufacturer "A" are a bit higher (but no more than 2.5%) than the typical value mentioned in the datasheet. Consequently, for a given material density, if all the dimensions are higher than the typical value, the weight should be higher and that's what we obtained. Nevertheless, the maximum and minimum values don't exceed more than 5% of the typical weight. The cores of manufacturer "B", give relatively different results. In fact, some measured average dimensions (a, b, c and f) are inferior to the datasheet typical value. Dimensions "a", "b", "c" are about 2% less than the typical value. Surprisingly dimension "f" (which is the ribbon width) is about 5% less than the typical value, with an error bar very small. Indeed, the ribbon width is normally a direct consequence of the manufacturing process (rapidly quenched technology), which is normally very reliable. This is not the case for dimension "f" of Manufacturer "A" cut cores which is very close to its datasheet value. Finally, in [8], it is said that the dimension "f" is always higher than the ribbon width, due to non alignment of subsequent layers in the core winding. Finally, dimensions "e" and "g" are a bit higher than the typical value.

B. Geometric dimensions analysis and discussion

One can see first that both manufacturers haven't made the same choices in terms of geometric tolerances. In order to analyse these choices, we introduce the new variables below :

- $W_a \propto e \cdot g$ is the core window area
- $A_e \propto c \cdot f$ is the effective iron cross section area

- $A_p \propto W_a \cdot A_e$ is the area product

The last variable A_p is very important when designing a transformer, because it can be shown that $A_p \propto P_t$, with P_t, the power handling capability. Manufacturer "A" cores have all their dimensions superior to the typical values. It leads to have A_p superior to its typical and calculated value and ensures that the real core can handle P_t. Manufacturer "B" cores have their "e" and "g" dimensions superior to their typical values, it leads to have W_a superior to its calculated value, whereas "f" and "g" are inferior to their typical values, which leads to have A_e inferior to its typical value. A_p is therefore an average of W_a and A_p and realises a compromise between these two variables in order that A_p is closed to its calculated value. Both manufacturers underestimate the weight.

III. MAGNETIC PROPERTIES

A. Measurement set-up

In the DAB1 topology, the magnetization is forced on one side of the transformer by a symmetrical square voltage waveform ($\alpha = 0.5$). This voltage implies a triangular waveform of the flux density. To measure B(H) curves, adapted to this operation, a dedicated test bench have been set-up. The principle is to measure electrical parameters on an adapted transformer and to extract magnetic magnitudes ($B(t)$ and $H(t)$). Two coils made of 15 turns each are wound on sample cores. In no load operation, the H field is directly obtained using the primary input current $I_1(t)$ and number of turns (n_1) and the mean path length (MPL) of the core (1). The secondary winding (n_2 turns) is used as a *"flux sensor"* and the B field is calculated using the voltage variation across it (2). The square voltage is made by a 1.2 kV IGBT 1-phase inverter that is powered by a source with an output voltage adjustable from 0 to 1 kV. A given operating point is set by selecting the proper frequency and maximum induction. The operating frequency range of the target application is from 8 to 50 kHz. The maximum induction in the core is set by the input voltage of the inverter and is in the range of 0.1 to 1.1 T.

$$H(t) = \frac{n_1 . I_1(t)}{MPL} \quad (1)$$

$$B(t) = \frac{\int V_2(t)}{n_2 . A_e} \quad (2)$$

The secondary voltage is measured with a passive high voltage probe – Lecroy PPE007 – plugged in a high speed oscilloscope – Lecroy Wavepro 725i –. The primary current is measured with a – Lecroy CP030 – closed loop hall effect sensor isolated current sensor. In order to compute the magnetic losses with $B(H)$ curve area, the primary current and the secondary voltage measurements have to be synchronized. According to [9], we compensated the delay of the current probe (13 ns) by setting the deskew function on the oscilloscope.

B. B(H) loops

We imposed triangular waveforms of B at different levels and different frequencies in order to measure the amplitude permeability μ_a and the magnetic losses p_{fe}. In this section, we only present measurement results for $B_{max} = 0.4$ T, $f = 20$ kHz and $T_{core} = 90$ °C for two reasons. First, the other results lead to the same conclusions. Second, this point is close to the foreseen operating point. The figures 3 and 4 show the $B(H)$ loops of "Manufacturer A" and "Manufacturer "B" respectively. In each figure, the black points loop represent the average behaviour of the cores (average $B(H)$ loop of all the cores), the cyan loop represent the "worst" loop in terms of permeability (lowest μ_a) and the magenta loop represent the "worst" loop in terms of losses (highest p_{fe}).
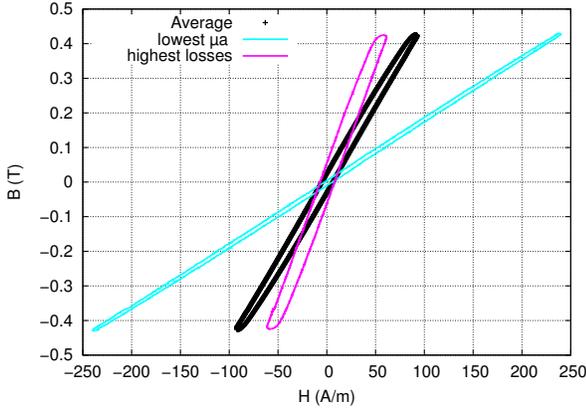
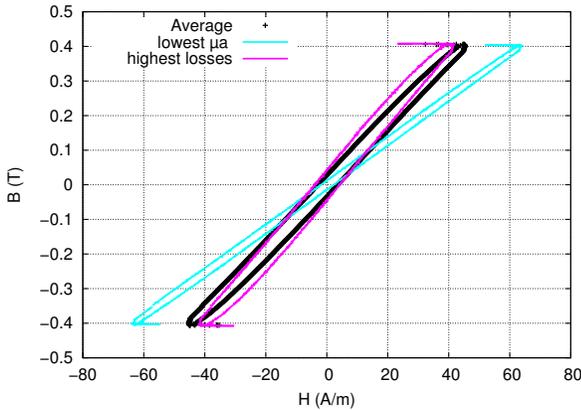Fig. 3. $B(H)$ loops for Manufacturer 'A'

Fig. 4. $B(H)$ loops for Manufacturer 'B'

C. μ_a and p_{fe} dispersion

With all the loops of each core, we determine the amplitude permeability μ_a and the specific magnetic losses p_{fe}. Figure 5 shows on the left the histograms of the relative amplitude permeability μ_a and the magnetic losses p_{fe} on the right for each manufacturer. The error bar on each histogram represents the maximum and minimum value measured for the complete set.
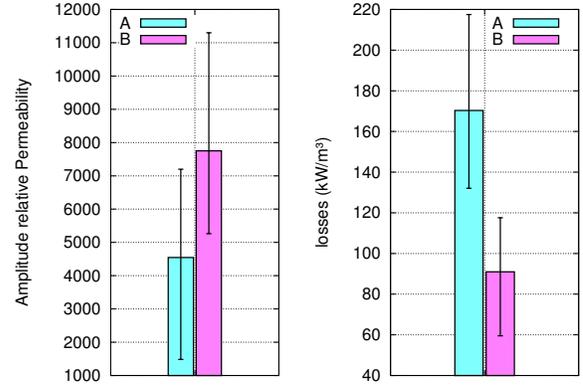
Fig. 5. Average, maximum and minimum values of relative amplitude permeability μ_a (left) and magnetic losses p_{fe} (right)

It is clear that the manufacturer 'A' cut-cores have a lower μ_a than those of the manufacturer 'B'. The ratio of the average values of $\mu_a(B)/\mu_a(A) \approx 1.7$. It means that a coil wound on an equivalent cross-section (of the same value) fed with the same voltage level would give a no load current ratio $I_0(A)/I_0(B) \approx 1.7$. It is also clear that manufacturer 'A' cut cores have much more magnetic losses than the manufacturer 'B' ones. Indeed, the ratio of magnetic losses $p_{fe}(A)/p_{fe}(B) \approx 2$. These two simple magnetic properties show that a hypothetical transformer made with manufacturer 'A' cut-cores would have much more no load losses (copper and magnetic losses) than a transformer with manufacturer 'B' cut-cores. In order to compare all the cut-cores and to show the dispersion of the previous mentioned parameters, we plot in figure 6, the cut cores coordinates in the $\mu_a - p_{fe}$ plane.
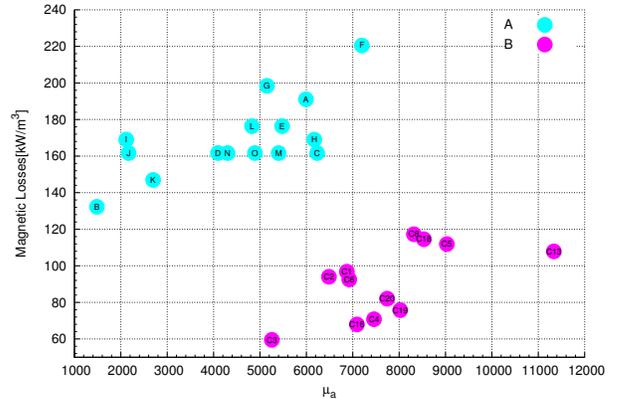
Fig. 6. Comparison of magnetic losses vs μ_a dispersion for the two manufacturers

The figures 5 and 6 clearly show that the dispersion of both magnitudes (μ_a and p_{fe}) is very high for both manufacturers. This dispersion is a big drawback for designers that need to be sure of the magnetic properties in order to design new products. Indeed, nanocrystalline cut cores are expensive compared to conventional ferrite cut cores. Despite their excellent magnetic properties, a too big dispersion of these properties could lead to not use them for new products.

Despite this dispersion, it is clear that the manufacturer 'B' cut cores are better than the manufacturer 'A' ones. We chose the representative "C2" core to make several measurements of losses in different operating conditions and developed a new model based on the improved generalised Steinmetz equation (iGSE) to take into account the temperature.

D. iGSE with temperature

We use the improved generalized Steinmetz equation (iGSE) model presented in [10] which has recently been improved in [11] to take into account relaxation effects. The last model isn't useful for us because we won't have relaxation effects in our cores (pure trangle waveforms). All these models have the assumption that the temperature of the core is constant. We decided to modify the iGSE model to take into account the temperature. We call this model the improved generalized Steinmetz equation with temperature (iGSET). p_{fe} are computed by solving (3).

$$p_{fe} = \frac{1}{T} \int_0^T k_i(T_e) \left| \frac{dB}{dt} \right|^\alpha (\Delta B)^{\beta-\alpha} dt \qquad (3)$$

with ΔB the peak to peak flux density and T_e the temperature. Only k_i depends on temperature. It is computed by (4) :

$$k_i(T_e) = \frac{k_0 + k_1 \cdot T_e + k_2 \cdot T_e^2}{(2\pi)^{\alpha-1} \int_0^{2\pi} |\cos\theta|^\alpha \, 2^{\beta-\alpha} d\theta} \qquad (4)$$

The identified parameters are summarized in the table I.

TABLE I
iGSET MODEL PARAMETERS

k_0	k_1	k_2	α	β
$2.08\cdot10^{-4}$	$3.97\cdot10^{-6}$	$-4.13\cdot10^{-8}$	1.63	2.16

In [11], the authors find values ($\alpha = 1.88$ and $\beta = 2.02$) for a nanocrystalline material. But, as it is showed in our paper, there is a big dispersion regarding the losses values. It is therefore very difficult to discuss and compare the α and β values. This last point requires further investigations. The figure 7 show the evolution of the losses p_{fe} vs the temperature for different levels of B (with triangular waveforms) at the frequency of 20 kHz.

The average relative mean square error between measurements and iGSET model is about 6.8%. The model can be further improved by increasing the measured temperatures until the limit of 155 ° C (class F products).

IV. CONCLUSION

Many nanocrystalline cut-cores have been measured (geometric dimensions) and characterized (magnetic properties). The two manufacturers haven't made the same choices in terms of geometric dimensions. Both of them approximately respect the datasheet, (except manufacturer 'B' for 'f' dimension). Both of them underestimate the weight of their
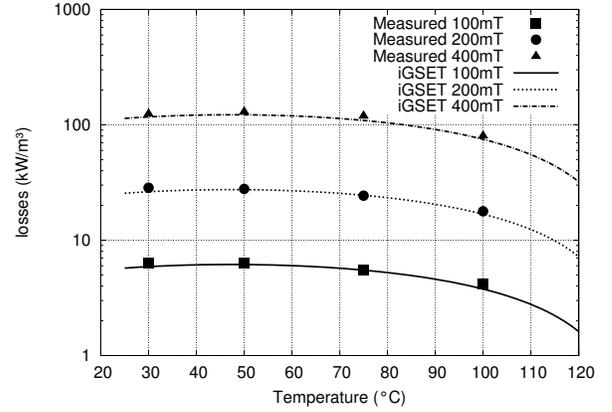

Fig. 7. losses vs temperature for different B levels at the frequency of $20kHz$

cores. The measured magnetic properties show that both manufacturers have a big dispersion in terms of amplitude permeability μ_a and on magnetic losses p_{fe}. Despite this dispersion, measurements show that manufacturer 'B' cores were a better choice in order to build a transformer. Finally an attempt to take into account the temperature in the improved general Steinmetz equation model (iGSET) has been realized. The iGSET model is in good agreement with measurements and further improvements can be made in terms of accuracy or temperature range.

REFERENCES

[1] Y. Yoshizawa, S. Oguma, and K. Yamauchi, "New fe-based soft magnetic alloys composed of ultrafine grain structure," *Journal of Applied Physics*, vol. 64, no. 10, pp. 6044–6046, 1988.
[2] A. Roc'h and F. Leferink, "Nanocrystalline core material for high-performance common mode inductors," *IEEE Transactions on Electromagnetic Compatibility*, vol. 54, no. 4, pp. 785–791, 2012.
[3] C. Sullivan and A. Muetze, "Simulation model of common-mode chokes for high-power applications," *IEEE Transactions on Industry Applications*, vol. 46, no. 2, pp. 884–891, 2010.
[4] T. Chailloux, M. Raulet, C. Martin, C. Joubert, F. Sixdenier, and L. Morel, "Magnetic behavior representation taking into account the temperature of a magnetic nanocrystalline material," *IEEE Transactions on Magnetics*, vol. 48, no. 2, pp. 455–458, 2012.
[5] Y. Shindo, T. Yoshihara, M. Otsubo, and M. Sawada, "A magnetic amplifier using nanocrystalline soft magnetic material," in *Power Electronics and ECCE Asia (ICPE, ECCE), 2011 IEEE 8th International Conference on*, May-Jun, 30-3, 2011, pp. 1299–1306.
[6] T. C. Batista, B. Luciano, R. Freire, and S. Catunda, "Current transformer with nanocrystalline alloy core for measurement," in *Instrumentation and Measurement Technology Conference (I2MTC)*, Binjiang, China, 2011, pp. 1–4.
[7] B. Cougo and J. Kolar, "Integration of leakage inductance in tape wound core transformers for dual active bridge converters," in *Integrated Power Electronics Systems (CIPS), 2012 7th International Conference on*, Nuremberg, GERMANY, 6-8, 2012, pp. 1–6.
[8] S. Zurek, "Differences in parameters of ni-fe wound toroidal cores supplied by industrial manufacturers," *IEEE Transactions on Magnetics*, vol. 48, no. 4, pp. 1371–1374, 2012.
[9] Lecroy products website. [Online]. Available: http://teledynelecroy.com/
[10] K. Venkatachalam, C. Sullivan, T. Abdallah, and H. Tacca, "Accurate prediction of ferrite core loss with nonsinusoidal waveforms using only steinmetz parameters," in *Computers in Power Electronics, 2002. Proceedings. 2002 IEEE Workshop on*, June 2002, pp. 1–4.
[11] M. Jonas, B. Jurgen, K. J. Walter, and E. Andreas, "Improved core-loss calculation for magnetic components employed in power electronic systems," *IEEE Transactions on Power Electronics*, vol. 27, no. 2, pp. 964–973, 2012.